

**Low-lying isomeric levels in  $^{75}\text{Cu}$** 

J. M. Daugas,<sup>1</sup> T. Faul,<sup>1</sup> H. Grawe,<sup>2</sup> M. Pfützner,<sup>3</sup> R. Grzywacz,<sup>4,5</sup> M. Lewitowicz,<sup>6</sup> N. L. Achouri,<sup>7</sup> J. C. Angélique,<sup>7</sup> D. Baiborodin,<sup>8</sup> R. Bentida,<sup>9</sup> R. Béraud,<sup>9</sup> C. Borcea,<sup>10</sup> C. R. Bingham,<sup>4</sup> W. N. Catford,<sup>11</sup> A. Emsallem,<sup>9</sup> G. de France,<sup>6</sup> K. L. Grzywacz,<sup>4</sup> R. C. Lemmon,<sup>12</sup> M. J. Lopez Jimenez,<sup>6</sup> F. de Oliveira Santos,<sup>6</sup> P. H. Regan,<sup>11</sup> K. Rykaczewski,<sup>5</sup> J. E. Sauvestre,<sup>1</sup> M. Sawicka,<sup>3</sup> and M. Stanoiu<sup>6,10</sup>

<sup>1</sup>CEA, DAM, DIF, F-91297 Arpajon cedex, France

<sup>2</sup>GSI-Helmholtzzentrum für Schwerionenforschung, Planckstrasse 1, D-64220 Darmstadt, Germany

<sup>3</sup>IEP, Warsaw University, 00681 Warsaw, PL-00681 Hoza 69, Poland

<sup>4</sup>Department of Physics and Astronomy, University of Tennessee, Knoxville, Tennessee 37996, USA

<sup>5</sup>Physics Division, Oak Ridge National Laboratory, Oak Ridge, Tennessee 37831, USA

<sup>6</sup>Grand Accélérateur National d'Ions Lourds (GANIL), CEA/DSM-CNRS/IN2P3, BP 55027, F-14076 Caen cedex 5, France

<sup>7</sup>Laboratoire de Physique Corpusculaire ENSICAEN, CNRS-IN2P3 UMR 6534 et Université de Caen, F-14050 Caen cedex, France

<sup>8</sup>Nuclear Physic Institute, CZ-25068 Rez, Czech Republic

<sup>9</sup>Institut de Physique Nucléaire de Lyon, CNRS/IN2P3, Université Lyon 1, F-69622 Villeurbanne cedex, France

<sup>10</sup>Horia Hulubei National Institute of Physics and Nuclear Engineering, P.O. Box MG6, Bucharest-Margule, Romania

<sup>11</sup>Department of Physics, University of Surrey, Guildford, GU2 5XH, United Kingdom

<sup>12</sup>CCLRC Daresbury Laboratory, Daresbury, Warrington, Cheshire, WA4 4AD, United Kingdom

K. Sieja<sup>2,13,14</sup> and F. Nowacki<sup>14</sup>

<sup>13</sup>Institut für Kernphysik, Technische Universität Darmstadt, D-64289 Darmstadt, Germany

<sup>14</sup>Institut Pluridisciplinaire Hubert Curien, 23 rue du Loess, BP28, F-67037 Strasbourg, France

(Received 14 December 2009; published 10 March 2010)

Isomeric low-lying states were identified and investigated in the  $^{75}\text{Cu}$  nucleus. Two states at 61.8(5)- and 128.3(7)-keV excitation energies with half-lives of 370(40)- and 170(15)-ns were assigned as  $^{75m1}\text{Cu}$  and  $^{75m2}\text{Cu}$ , respectively. The measured half-lives combined with the recent spin assignment of the ground state allow one to deduce tentatively spin and parity of the two isomers and the dominant multipolarities of the isomeric transitions with respect to the systematics of the Cu isotopes. Shell-model calculations using an up-to-date effective interaction reproduce the evolution of the  $1/2^-$ ,  $3/2^-$ , and  $5/2^-$  states for the neutron-rich odd-mass Cu isotopes when filling the  $\nu g_{9/2}$ . The results indicate a significant change in the nuclear structure in this region, where a single-particle  $5/2^-$  state coexists with more and more collective  $3/2^-$  and  $1/2^-$  levels at low excitation energies.

DOI: [10.1103/PhysRevC.81.034304](https://doi.org/10.1103/PhysRevC.81.034304)

PACS number(s): 23.35.+g, 23.20.Lv, 21.10.Tg, 21.60.Cs

**I. INTRODUCTION**

Experimental evidence of the evolution of nuclear structure along an isotopic or isotonic chain is an essential ingredient to have a better understanding of the nucleon-nucleon interaction. In this context, one of the major activities in nuclear structure is the search for appearance and disappearance of magic numbers revealing the evolution of shell structure toward the drip lines. In particular, the region of neutron-rich nuclei around  $N = 40$  to  $N = 50$  shows an interesting evolution of shell structure. It is well known that a transition from harmonic oscillator to spin-orbit type of shell closure occurs between  $^{40}\text{Ca}$  and  $^{100}\text{Sn}$  and the role of the neutron  $g_{9/2}$  orbital becomes crucial in the vicinity of  $^{68}\text{Ni}$ , determining its mixed, magic and superfluid, character [1]. In nuclei with a proton number below and above the nickel isotopes, the neutron  $g_{9/2}$  orbital manifests itself as low-lying isomeric states already at  $N = 35$ , namely  $^{63}\text{Ni}$ ,  $^{61}\text{Fe}$ , and  $^{59}\text{Cr}$ , and it induces important excitations across the  $Z = 28$  shell gap, for example, in  $^{65}\text{Ni}$  [2]. Most of the neutron-rich Cu isotopes show predominant single-particle character of their low-lying states. For example, in  $^{69}\text{Cu}$  the transition probabilities for these states are well reproduced

using a  $^{56}\text{Ni}$  core and conventional effective charges. However, to explain the properties of the neighboring  $^{67}\text{Cu}$  and  $^{71}\text{Cu}$ , one needs either to increase the model space to a  $^{48}\text{Ca}$  core including the proton  $\pi f_{7/2}$  orbit or allow much larger effective charges [3]. With the increase of the occupation of the  $\nu g_{9/2}$  orbital its influence on the structure of the nuclei becomes more important, causing a significant decrease of the energy gap between the proton  $f_{7/2}$  and  $f_{5/2}$  orbitals, usually referred to as monopole migration [4,5]. As a consequence for  $^{73}\text{Cu}$  one observes a coexistence of collective and single-particle-like states at very low excitation energy [6]. It has been debated whether and at what neutron number a crossing of the  $\pi f_{5/2}$  and  $\pi p_{3/2}$  should occur [7–10], and what might be its influence on the doubly magic character of  $^{78}\text{Ni}$ . If confirmed in nuclei toward  $N = 50$ , see, e.g., Ref. [11], the monopole migration of the  $\pi f_{5/2}$  orbital could eventually erode the magic character of the  $Z = 28$  shell closure, which would then be built on the  $\pi f_{7/2}$  and  $\pi f_{5/2}$  orbits. Depending on the strength of the proton-neutron interaction,  $^{78}\text{Ni}$ , where the  $\nu g_{9/2}$  orbital is fully occupied, and hence the monopole interaction maximized, could reveal magic character or not [12].

The excitation energy of the  $5/2^-$  state along the odd-mass Cu isotopes remains rather constant up to  $N = 40$ , above 1 MeV, and decreases drastically when the  $\nu g_{9/2}$  orbital starts to be filled. It drops to 534 and 166 keV for the  $^{71}\text{Cu}$  and  $^{73}\text{Cu}$ , respectively. The sharp drop of the excitation energy of the  $5/2^-$  state beyond  $N = 40$  is caused by the lowering of the  $\pi f_{5/2}$  state with respect to the  $\pi p_{3/2}$  ground state when neutrons start filling the  $g_{9/2}$  orbital [4,7,8,10]. Recently, the  $g$ -factor measurement of the ground state of the  $^{75}\text{Cu}$  unambiguously shows the  $\pi f_{5/2}$  character of this state, assigning a  $5/2^-$  spin and parity [13]. The excitation energy of the  $1/2^-$  state beyond  $N = 40$  has the same slope as that of the  $5/2^-$ , dropping from 1 MeV down to 454.2 and 135.4 keV for the  $^{71}\text{Cu}$  and  $^{73}\text{Cu}$ , respectively. The observed increased  $B(E2; 1/2^- \rightarrow 3/2^-)$  value indicates significant collectivity of this state. However, low-lying states and reduced transition probabilities  $B(E2)$  are known only up to  $N = 44$ . In this work, the first experimental information about the transition rates at  $N = 46$  is obtained.

## II. EXPERIMENTAL PROCEDURE

The present experiment aimed at the search and study of new isomeric states in the neutron-rich region from potassium to germanium isotopes. Those isotopes were produced by the fragmentation reaction of a  $^{86}\text{Kr}$  beam at intermediate energy. This experiment is a continuation of a previous one where 13 isomeric states have been observed and studied for the first time [14]. Ten new isomeric states have been observed in the present work [15] thanks to the increase of the primary beam intensity, reduction of fragments time of flight by a factor 6 (from 1.2  $\mu\text{s}$  to 200 ns) and detection of low-energy  $\gamma$  rays. In particular, the observation of the  $8^+$  isomeric state in  $^{78}\text{Zn}$  [16] gave the first experimental information on the shell structure very close to the doubly magic  $Z = 28$ ,  $N = 50$  nucleus  $^{78}\text{Ni}$ .

The experiment has been performed at Grand Accélérateur National d'Ions Lourds (GANIL) using the LISE spectrometer [17]. The short-lived isomers were produced using the fragmentation reaction of a 60.5 MeV per nucleon neutron-rich stable  $^{86}\text{Kr}^{34+}$  beam impinging on a rotating 100- $\mu\text{m}$  thick  $^{\text{nat}}\text{Ni}$  target. The mean intensity of the primary beam was about 1.6  $\mu\text{Ae}$ , which corresponds to  $3 \times 10^{11}$  particles per second. Behind the production target a 500- $\mu\text{m}$  thick Be foil was used as a stripper. In the first dispersive plane of the spectrometer located in between the two selective dipoles, was placed a 50- $\mu\text{m}$  thick Be wedge to remove light fragments and to further suppress non-fully stripped ions. The produced fragments were detected by a three-element Si-detector telescope of 300-, 300-, and 500- $\mu\text{m}$  thickness, respectively. The third one is a position-sensitive detector that was mounted at an angle of  $45^\circ$  with respect to the beam axis. The heavy ions were implanted in the middle of this silicon detector. Four high-purity germanium detectors surrounded the implantation Si-detector in a close geometry. The total photopeak efficiency was measured to be maximum 26% at 130 keV and 6.2(1)% for 1.3-MeV  $\gamma$  rays.

The unambiguous identification of heavy ions in mass, atomic number, and atomic charge was achieved by means of

energy-loss, total-kinetic-energy, and time-of-flight measurements. A detailed description of the experimental method used for the identification and studies of short-lived isomers can be found in Ref. [18]. The heavy-ion delayed  $\gamma$ -ray correlation applied event by event allows an independent confirmation of fragment identification. The lifetimes of isomeric states were measured by storing the time difference between the heavy-ion implantation signal and delayed  $\gamma$  rays. Two separate time ranges of up to 500 ns and 40  $\mu\text{s}$  were recorded for each germanium crystal using standard time-to-digital converter (TDC) and time-to-amplitude converter (TAC) modules, respectively.

## III. RESULTS AND DISCUSSION

A summary of the measured  $\gamma$  rays and half-lives for new isomeric states observed in this experiment is presented in Table I. In the present report, only results concerning the isomeric states in  $^{75}\text{Cu}$  will be discussed.

In Fig. 1 the delayed  $\gamma$ -ray spectrum gated on the implantation of  $^{75}\text{Cu}$  is displayed. This energy spectrum is obtained by the summation of all germanium detectors' contributions. Two  $\gamma$  rays have been clearly observed at the energies of 61.8(5) and 66.5(5) keV. One observes that the two  $\gamma$  rays are in coincidence. The timing spectra reveal two different half-lives, which means that the higher energy isomeric state decays to the lower energy one. The time decay patterns of the isomeric transitions are shown in the inset of Fig. 1. An exponential  $\chi^2$  fit to the experimental histogram gives a half-life value of 170(15) ns for the 66.5(5)-keV  $\gamma$ -ray transition shown in Fig. 1(a). Concerning the half-life of the lower energy isomer,

TABLE I. List of new isomers observed in the present experiment. Given are  $E^*$ , deduced excitation energy;  $T_{1/2}$ , half-life;  $I^\pi$ , tentative spin assignment of the isomeric state; Mult, multipolarity of the isomeric transition; and  $E_\gamma$ , energies of the observed  $\gamma$  lines. For the cases marked with (\*); a new  $\gamma$  transition is observed. For the  $^{78}\text{Ga}$ , only the isomeric transitions are given.

	$E^*$ (keV)	$T_{1/2}$ (ns)	$I^\pi$	Mult.	$E_\gamma$ (keV)
$^{50}\text{K}$	171.4	125(40)	(3 $^-$ )	$E2$	44, 70, <b>101</b> <b>127.4, 171.4</b>
$^{60m1}\text{V}$	103.2	13(3)	(2 $^+$ )	$M1 + E2$	<b>103.2</b>
$^{60m2}\text{V}$	202.1	320(90)	(4 $^+$ )	$E2$	<b>98.9</b> , 103.2
$^{62}\text{Mn}$	113.3	95(2)		$M1 + E2$	<b>113.3</b>
$^{64}\text{Mn}^*$	174.1	>100 $\mu\text{s}$	(4 $^+$ )	$M2$	39.8, <b>134.3</b>
$^{65}\text{Fe}^*$	396.8	420(13)			<b>33.5</b> , 363.3
$^{67}\text{Fe}^*$	>387.7	62(23) $\mu\text{s}$			366.4, 387.7
$^{68}\text{Co}$	48.4	101(10)			<b>48.4</b>
$^{70}\text{Co}$	437.3	54(10)	(4 $^-$ )	$E1 + M2$ $E2$	<b>155.8</b> <b>273.2</b> , 164.1
$^{75m1}\text{Cu}$	61.8	370(40)	(1/2 $^-$ )	$E2$	<b>61.8</b>
$^{75m2}\text{Cu}$	128.3	170(15)	(3/2 $^-$ )	$M1 + E2$	<b>66.5</b>
$^{78}\text{Zn}$	2672.5	319(9)	8 $^+$	$E2$	<b>144.7</b> , 729.6 889.9, 908.3
$^{78}\text{Ga}$	498.9	110(3)			<b>46.1</b> , <b>157.5</b> <b>217.8, 498.9</b>

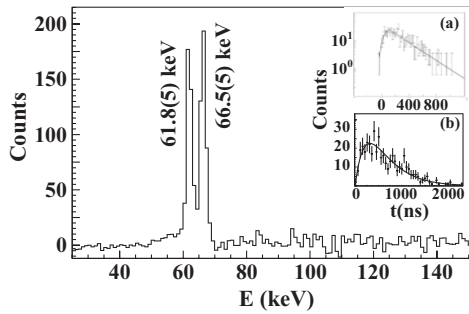


FIG. 1. The  $\gamma$ -ray energy spectrum of the isomeric state in  $^{75}\text{Cu}$ . The decay curves of both observed transitions are shown in the inset for the 66.8(5)-keV (a) and 61.8(5)-keV (b)  $\gamma$  rays, note the different timescales.

the feeding component from the upper one was determined from a two-component fit of the 61.8(5)-keV decay curve. It turns out that the lower isomeric state was almost fully fed by the decay of the upper isomer. For the exponential fit of the decay of the first isomeric state, 100% feeding is assumed. The fitted half-life presented in Fig. 1(b) gives 370(40) ns. No direct transition from the level at an excitation energy of 128.3(7) keV to the ground state is observed. Thus, two low-lying isomeric states were measured in the  $^{75}\text{Cu}$ ; the first one, namely  $^{75m1}\text{Cu}$ , is located at an excitation energy of 61.8(5) keV with a half-life of 370(40) ns and the second one, namely  $^{75m2}\text{Cu}$ , at an excitation energy of 128.3(7) keV with a 170(15)-ns half-life.

The reduced transition strengths, expressed in Weisskopf units (W.u.), assuming pure  $E2$  and  $M1$  multiplicities, respectively, are  $B(E2) = 35(5)$  W.u.,  $B(M1) = 3.8(4) \times 10^{-4}$  W.u. for the 66.5(5)-keV isomeric transition, and  $B(E2) = 19(3)$  W.u.,  $B(M1) = 2.1(3) \times 10^{-4}$  W.u. for the 61.8(5)-keV isomeric transition. Internal conversion coefficients [19]  $\alpha_{\text{tot}}(E2) = 2.85(10)$ ,  $3.76(13)$  and  $\alpha_{\text{tot}}(M1) = 0.163(5)$ ,  $0.200(6)$  for the 66.5(5)- and 61.8(5)-keV  $\gamma$  rays, respectively, were used in the calculation. For the 128.3(7)-keV crossover transition, internal conversion coefficients are evaluated to be  $\alpha_{\text{tot}}(E2) = 0.238(6)$  and  $\alpha_{\text{tot}}(M1) = 0.0276(5)$ . According to these values and to the measured  $\gamma$  efficiency, one estimates the nonobserved crossover transition to be lower than 3% leading to reduced transition strengths

TABLE II. Experimental excitation energies (keV) of the  $3/2^-$ ,  $1/2^-$ , and  $5/2^-$  levels and the corresponding  $B(E2)$ ,  $B(M1)$  values (expressed in Weisskopf units) extracted from the analysis of previous and present data (Expt.) compared to the results of the large shell-model calculations (SM). The shell-model  $B(E2)$  values are calculated with the effective charge  $e_\nu = 0.5e$  and  $e_\pi = 1.5e$ . For the  $B(M1)$  values, effective gyromagnetic factors were used; see text for details.

	$^{69}\text{Cu}$		$^{71}\text{Cu}$		$^{73}\text{Cu}$	
	Expt.	SM	Expt.	SM	Expt.	SM
$E(3/2^-)$	0	0	0	0	0	0
$E(1/2^-)$	1096	1052	454.2(1)	715	135.4(1)	262
$E(5/2^-)$	1214	1142	534	763	166	231
$B(E2; 1/2^- \rightarrow 3/2^-)$	10.4(10)	7.6	20.4(22)	10.8	23.1(21)	13.3
$B(E2; 3/2^- \rightarrow 5/2^-)$	4.5(11)	6.2	5.9(18)	7.9	6.6(27)	3.9

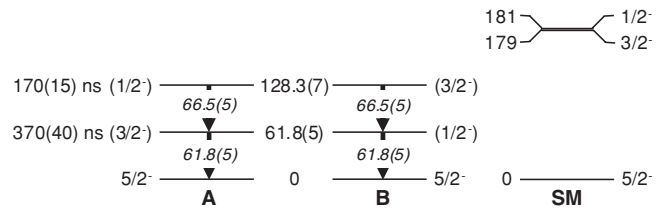


FIG. 2. Proposed experimental spin assignment scenarios A and B compared with SM calculations.

of  $B(E2) < 0.16$  W.u. and  $B(M1) < 2.1 \times 10^{-6}$  W.u. assuming pure  $E2$  and  $M1$  multipolarity, respectively.

With respect to the experimental low-lying level energies systematics study on the copper isotopes shown in Table II (Expt.), the spin assignment to the two isomeric states may be discussed in terms of two scenarios. The recent determination of the  $5/2^-$  ground-state spin and parity [13] leads to  $1/2^-$  and  $3/2^-$  low-lying possible states. Depending on the migration of these latter relative to the  $5/2^-$  level along the neutron-rich Cu isotopes, their order in  $^{75}\text{Cu}$  could follow two possibilities, hereafter referred to as A and B in Fig. 2. As the neutron number increases, the gap between the  $5/2^-$  and  $1/2^-$  states decreases from 118 keV in  $^{69}\text{Cu}$  to 80 keV in  $^{71}\text{Cu}$  down to 31 keV in  $^{73}\text{Cu}$ , and the gap between  $1/2^-$  and  $3/2^-$  states is reduced from 1096 keV for  $A = 69$  to 454 keV for  $A = 71$  and finally to 135 keV for  $A = 73$ . According to the systematics, the previous gaps are awaited to be  $-25$ - and  $-30$ -keV for the  $^{75}\text{Cu}$ , respectively. Within the framework of scenario A, the gap between the three above-mentioned states becomes  $-128$  keV and 66 keV, and these latter are reduced to  $-62$  keV and to  $-66$  keV if there is a  $5/2^-$  (g.s.)- $1/2^-$  ( $m1$ )- $3/2^-$  ( $m2$ ) sequence (scenario B). In comparison with the energy gap evolution, the second proposition seems more credible.

To shed light on the nuclear structure of the low-energy states of the  $^{75}\text{Cu}$ , the experimental results have been contrasted with large-scale shell-model (SM) calculations performed in a valence space outside the  $^{48}\text{Ca}$  core, comprising  $f_{7/2}$ ,  $f_{5/2}$ ,  $p_{3/2}$ ,  $p_{1/2}$  orbitals for protons and  $f_{5/2}$ ,  $p_{3/2}$ ,  $p_{1/2}$ ,  $g_{9/2}$  for neutrons. As already mentioned, such a model space appears to be indispensable for a proper description of the nuclear structure of neutron-rich nuclei in this region: it was shown by Otsuka in Ref. [20] that a strong proton-neutron tensor force has an opposite action on the  $\pi f_{7/2}$  and  $\pi f_{5/2}$

TABLE III. Transition rates in proposed scenarios expressed in W.u. for  $^{75}\text{Cu}$ . Only upper limits are given because of unknown mixing ratios. Experimental reduced transition probability for the two new  $\gamma$  rays are corrected by internal conversion coefficients assuming pure  $E2$  and  $M1$  transitions.

$E_\gamma$	Transition	Multipolarity	Scenario A	Scenario B	SM
61.8	$3/2^- \rightarrow 5/2^-$	$E2$	$<19(3)$		3.35
		$M1$	$<2.1(3) \times 10^{-4}$		0.009
61.8	$1/2^- \rightarrow 5/2^-$	$E2$		19(3)	19.9
66.5	$1/2^- \rightarrow 3/2^-$	$E2$	$<35(5)$		14.5
		$M1$	$<3.8(4) \times 10^{-4}$		0.047
66.5	$3/2^- \rightarrow 1/2^-$	$E2$		$<35(5)$	7.25
		$M1$		$<3.8(4) \times 10^{-4}$	0.0235
128.3	$1/2^- \rightarrow 5/2^-$	$E2$	$<0.16$		19.9
128.3	$3/2^- \rightarrow 5/2^-$	$E2$		$<0.16$	3.35
		$M1$		$<2.1 \times 10^{-6}$	0.009

orbitals while filling of the neutron  $g_{9/2}$  level, which may result in a weakening of the  $Z = 28$  gap. It should be noted though that this is partly counterbalanced by the central part of the  $NN$  interaction [21]. Hence, the proton excitations from the  $f_{7/2}$  orbital may become of crucial importance when approaching  $N = 50$ . Recent SM calculations [22], as well as the results of this work, seem to confirm this prediction.

The effective interaction used is based on the interaction applied in the study of the Coulomb excitation in  $^{68}\text{Ni}$  in Ref. [1], however, we have modified the  $f_{7/2}$ - $f_{5/2}$  proton gap in  $^{78}\text{Ni}$  to reproduce its size constrained by the recently measured  $B(E2; 2^+ \rightarrow 0^+)$  value in  $^{80}\text{Zn}$  [23]. The calculations have been carried out with the m-scheme code ANTOINE [24]. We have pursued truncated calculations up to eight particle-8 hole excitations with respect to the  $f_{7/2}$  and  $p_{1/2}$  shell closures for lighter coppers, whereas a full space diagonalization was achieved for  $^{79,77,75}\text{Cu}$ .

The results for low-lying excited levels and electromagnetic transition rates for 69–75 copper isotopes in comparison to experimental data [25] are collected in Tables II and III and Figs. 2 and 3. Conventional polarization charge  $0.5e$  has been used for both protons and neutrons. For magnetic transitions spin  $g$  factors were quenched by a factor of 0.75 and we have used values of 1.1 and  $-0.1$  for orbital proton and neutron  $g$  factors, respectively. With these values we have reproduced most accurately the measured magnetic moments along the copper chain [22].

As seen from Table II and Fig. 3, the SM calculations reproduce very well the systematics of the low-lying levels along the Cu chain. In particular, the observed inversion of the  $3/2^-$  and  $5/2^-$  levels has been obtained in the calculations in  $^{75}\text{Cu}$ , where the  $g_{9/2}$  orbital is half-filled. Apparently, the attraction between the  $g_{9/2}$  neutrons and the  $f_{5/2}$  protons pulls down the  $f_{5/2}$  orbital, which then crosses the  $p_{3/2}$ . One should also notice that the present shell-model calculations succeed in reproducing the pronounced lowering of the  $1/2^-$  level, which was not the case in previous SM calculations in more restricted valence spaces [7,12,26].

The character of the calculated levels can be verified by looking into the transition rates presented in Table III.

Experimentally, all  $M1$  transitions are highly retarded in either scenario. This is qualitatively reproduced by the shell model though the SM values still overestimate the strengths. This can be ascribed to their sensitivity to small components in the wave functions and to the choice of the effective  $g$  factors, because of interference effects. Although the small  $B(M1; 3/2^- \rightarrow 5/2^-)$  reflects  $l$ -forbiddance and partial persistence of the  $p_{3/2}$  and  $f_{5/2}$  single-particle character of the respective states, the hindrance of the  $3/2^- \rightarrow 1/2^-$   $M1$  transition clearly indicates a completely different intrinsic structure of the  $1/2^-$  state. A typical single-particle  $p_{1/2} \rightarrow p_{3/2}$  spin-flip  $M1$  strength corresponds to 0.3–0.5 W.u. as measured in  $^{59-65}\text{Cu}$  [25].

The experimental  $B(E2; 1/2^- \rightarrow 3/2^-)$  value is about 10 W.u. at  $N = 40$  and reaches more than 20 W.u. in  $^{73}\text{Cu}$ , pointing out an increasingly collective character of this transition. On the contrary, the  $B(E2; 3/2^- \rightarrow 5/2^-)$  value is of a few W.u. along the chain and together with an observation of a sharp drop in energy of the  $5/2^-$  state can be a hint

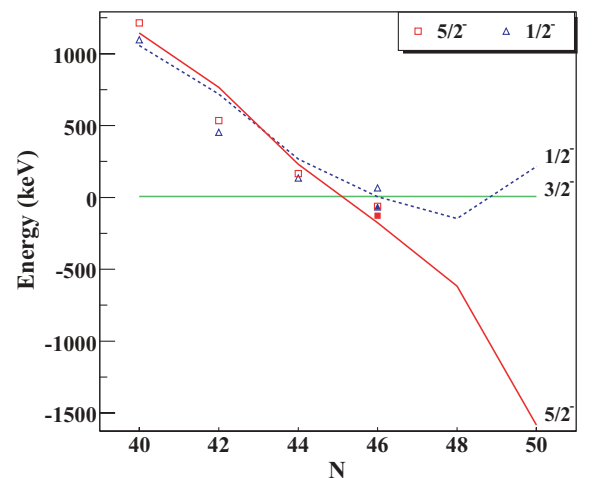


FIG. 3. (Color online) Evolution of the  $I^\pi = 1/2^-, 3/2^-,$  and  $5/2^-$  level energies from  $N = 40$ – $50$  in comparison to SM results. The open symbols represent the experimental data and the lines are for the calculated ones. The two scenarios for  $^{75}\text{Cu}$  ( $N = 46$ ) are indicated by open (A) and solid (B) symbols.

for the single-particle character of this state. The  $B(E2)$  strengths with standard polarization charge are satisfactorily reproduced within a factor of two by the shell model while the increasing trend is matched by the calculations. The noncollective  $B(E2; 3/2^- \rightarrow 5/2^-)$  value is fairly reproduced from  $^{69}\text{Cu}$  to  $^{73}\text{Cu}$  and remains of the same order in  $^{75}\text{Cu}$ , supporting the single-particle nature of the  $5/2^-$  level. The calculated wave function of this  $5/2^-$  is built up by  $\sim 65\%$  of the  $\pi f_{5/2}^1$  configuration. For comparison, the  $3/2^-$  and  $1/2^-$  states contain  $\sim 45\%$  and  $\sim 30\%$  of  $\pi p_{3/2}^1$  and  $\pi p_{1/2}^1$  components, respectively. These values reflect the gain in collectivity with the filling of the  $\nu g_{9/2}$  orbital.

The  $B(E2)$  values remain nearly indifferent to fine variations of polarization charges. We have also examined the sensitivity of calculated transitions in  $^{75}\text{Cu}$  to the size of the  $f_{7/2}-f_{5/2}$  proton gap. The reduction of the gap by 1 MeV, leads to the increase of  $B(E2)$  values by 3.5 W.u. for the  $1/2^- \rightarrow 3/2^-$  transition and by only 0.6 W.u. for the  $3/2^- \rightarrow 5/2^-$  one. Drawing on the fair agreement of the SM  $B(E2)$  values with experiment, the two scenarios for spin assignments are examined with respect to transition rates (see Table III). The upper limits extracted for the reduce strengths for the nonobserved 128-keV crossover transition are decisive to assess the two scenarios. In case A with a spin-parity sequence  $5/2^-$  (g.s.) -  $3/2^-(m1)$  -  $1/2^-(m2)$ , the upper limit of 0.16 W.u. for the  $1/2^- \rightarrow 5/2^-$  transition is largely contradicting the SM value of 19.9 W.u. whereas the limits of the observed  $E2$  transitions are compatible with both theory and systematics of the lighter copper isotopes. In scenario B and a sequence  $5/2^-$  (g.s.) -  $1/2^-(m1)$  -  $3/2^-(m2)$ , the enhanced  $E2$  transitions are well reproduced by the shell model whereas the hindered  $3/2^- \rightarrow 5/2^-$   $E2$  strength is overestimated. It should be noted that a pure  $\pi p_{3/2} \rightarrow \pi f_{5/2}$   $E2$  would correspond to 1.5 W.u. only (i.e., again small components in the wave function may cause destructive interference). In summary, the comparison of the experimental  $E2$  limits with shell-model results seems to favor scenario B in agreement with the systematics study. For the  $\Delta I=1$  transitions,  $E2/M1$  mixing ratios will improve the agreement for strong  $E2$  while at the same time the  $M1$  situation degrades; the general discussion, however, will be little affected. The situation resembles very much the antimony isotopes  $^{119-125}\text{Sb}$  one major shell higher in midshell  $\nu h_{11/2}$  where strong and weak  $E2$  are observed for the corresponding  $3/2^+ \rightarrow 5/2^+$ ,

$3/2^+ \rightarrow 7/2^+$ , and  $5/2^+ \rightarrow 7/2^+$ , respectively, while all  $M1$  are strongly hindered [25]. We note in passing that the kink at  $N = 48$  in the SM relative excitation energy trend shown in Fig. 3 indicates a return to single-particle behavior at the neutron shell closure  $N = 50$  in agreement with the spherical  $\nu g_{9/2}^-$  structure of  $^{76}\text{Ni}$  [27,28].

#### IV. CONCLUSION

In conclusion, we have observed the low-lying isomeric levels in  $^{75}\text{Cu}$  at excitation energies of 61.8(5) and 128.3(7) keV. The present experimental work triggered theoretical improvements in the description of the structure toward  $^{78}\text{Ni}$ . From comparison of the measured transition energies and deduced  $B(E2)$  values with the shell-model calculations the first spectroscopic information has been gained. The calculations describe correctly the observed isomeric states and support the experimental evidence for the inversion of  $p_{3/2}$  and  $f_{5/2}$  orbitals around  $^{75}\text{Cu}$  nucleus in agreement with the assignment of Flanagan *et al.* [13]. Two scenarios have been proposed for the assignment of the isomeric states. The systematics and SM calculations favor scenario B implying a  $(3/2^-)^{75m2}\text{Cu}$  decaying via a mixed  $M1 + E2$  transition and a  $(1/2^-)^{75m1}\text{Cu}$  feeding the  $5/2^-$  ground state by a pure  $E2$  multipolarity transition. The presence of single-particle and increasingly collective states at low excitation energy in the neutron-rich Cu isotopes in midshell  $\nu g_{9/2}$  reveal an interesting behavior in the nuclear structure evolution toward  $N = 50$  where according to the shell- model predictions the single-particle character of states should be recovered.

#### ACKNOWLEDGMENTS

We are grateful for the technical support provided to us by staff at the GANIL facility. We gratefully thank the Niels Bohr Institute (Copenhagen, Denmark) for providing a clover Ge detector. This work was partially supported by the POLONIUM project (Grant No. 98275), KBN (Grant No. 2P03B03615), US Department of Energy (Contract No. DE-AC05-96OR22464), and the Alliance (Grant No. 98029) between University of Surrey and GANIL and Engineering and Physical Sciences Research Council (United Kingdom). K.S. was supported by the state of Hesse within the Helmholtz International center for FAIR (HIC for FAIR) and the DFG (German Research Foundation) under Grant No. SFB 634.

[1] O. Sorlin *et al.*, Phys. Rev. Lett. **88**, 092501 (2002).  
 [2] G. Georgiev *et al.*, Eur. Phys. J. A **30**, 351 (2006).  
 [3] I. Stefanescu *et al.*, Phys. Rev. Lett. **98**, 122701 (2007).  
 [4] S. Franchoo *et al.*, Phys. Rev. Lett. **81**, 3100 (1998).  
 [5] S. Franchoo *et al.*, Phys. Rev. C **64**, 054308 (2001).  
 [6] I. Stefanescu *et al.*, Phys. Rev. Lett. **100**, 112502 (2008).  
 [7] N. A. Smirnova, A. De Maesschalck, A. Van Dyck, and K. Heyde, Phys. Rev. C **69**, 044306 (2004).  
 [8] A. F. Lisetskiy, B. A. Brown, and M. Horoi, Eur. Phys. A **25**, s01, 95 (2005).

[9] T. Niksić, T. Marketin, D. Vretenar, N. Paar, and P. Ring, Phys. Rev. C **71**, 014308 (2005).  
 [10] T. Otsuka, T. Suzuki, R. Fujimoto, H. Grawe, and Y. Akaishi, Phys. Rev. Lett. **95**, 232502 (2005).  
 [11] S. Ilyuskin *et al.*, Phys. Rev. C **80**, 054304 (2009).  
 [12] A. F. Lisetskiy, B. A. Brown, M. Horoi, and H. Grawe, Phys. Rev. C **70**, 044314 (2004).  
 [13] K. Flanagan *et al.*, Phys. Rev. Lett. **103**, 142501 (2009).  
 [14] R. Grzywacz *et al.*, Phys. Rev. Lett. **81**, 766 (1998).

- [15] M. Lewitowicz *et al.*, Nucl. Phys. **A654**, 687c (1999).
- [16] J. M. Daugas *et al.*, Phys. Lett. **B476**, 213 (2000).
- [17] R. Anne, D. Bazin, A. C. Mueller, J. C. Jacmart, and M. Langevin, Nucl. Instrum. Methods Phys. Res., Sect. A **257**, 215 (1987).
- [18] R. Grzywacz *et al.*, Phys. Lett. **B355**, 439 (1995).
- [19] T. Kibédi, T. W. Burrows, M. B. Trzhaskovskaya, P. M. Davidson, and C. W. Nestor Jr., Nucl. Instrum. Methods A **589**, 202 (2008).
- [20] T. Otsuka, T. Matsuo, and D. Abe, Phys. Rev. Lett. **97**, 162501 (2006).
- [21] T. Otsuka, T. Suzuki, M. Honma, Y. Utsuno, N. Tsunoda, K. Tsukiyama, and M. Hjorth-Jensen, Phys. Rev. Lett. **104**, 012501 (2010).
- [22] K. Sieja and F. Nowacki (to be published).
- [23] J. Van de Walle *et al.*, Phys. Rev. Lett. **99**, 142501 (2007).
- [24] E. Caurier and F. Nowacki, Acta Phys. Pol. B **30** 705 (1999).
- [25] ENSDF database, <http://www.nndc.bnl.gov/ensdf/>.
- [26] M. Honma, T. Otsuka, T. Mizusaki, and M. Hjorth-Jensen, Phys. Rev. C **80**, 064323 (2009).
- [27] M. Sawicka *et al.*, Eur. Phys. J. A **20**, 109 (2004).
- [28] C. Mazzocchi *et al.*, Phys. Lett. **B622**, 45 (2005).